Theoretical study of ferroelectric potassium nitrate

Oswaldo Diéguez* and David Vanderbilt
Department of Physics and Astronomy, Rutgers University, Piscataway, New Jersey 08854-8019, USA
(Dated: July 17, 2007)

We present a detailed study of the structural behavior and polarization reversal mechanism in phase III of KNO_3, an unusual ferroelectric material in which the nitrate groups rotate during polarization reversal. This material was one of several studied in a previous work [O. Diéguez and D. Vanderbilt, Phys. Rev. Lett. **96**, 056401 (2006)] where methods were described for computing curves of energy versus electric polarization. In the present work we extend and systematize the previous first-principles calculations on KNO_3, and analyze in detail a two-parameter model in which the energy of the system is written as a low-order expansion in the polarization and the nitrate group orientation. We confirm that this model reproduces the first-principles results for KNO_3 very well and construct its parameter-space phase diagram, describing regions where unusual triple-well potentials appear. We also present first-principles calculations of KNO_3 under pressure, finding that its energy-versus-polarization curves change character by developing a first-derivative discontinuity at zero polarization.

PACS numbers: PACS: 77.80.-e 81.05.Zx

I. INTRODUCTION

Potassium nitrate (KNO_3), also known as saltpetre, has long been used as an ingredient in explosives and propellants, including 'black powder' and other early forms of gunpowder. At room temperature and pressure, KNO_3 crystallizes in an aragonite (*Pnma*) phase with four formula units. This phase is usually referred to as phase II, and its domain of existence is illustrated in the phase diagram of Fig. 1 in Ref. 1. When this material is heated at atmospheric pressure, a transition to phase I occurs. The structure of phase I seems to have been the subject of a controversy for years, with the current status being not much changed since the discussion given twenty years ago by Scott *et al.* in Ref. 1. The proposed structure has global C_3 symmetry but local D_6 symmetry. Upon cooling at atmospheric pressure, phase I does not transform back to phase II; instead there is a narrow window of temperatures (aproximately from 113°C to 120°C) in which a ferroelectric phase, known as phase III, occurs. It is possible to broaden the range of temperatures in which phase III exists by applying hydrostatic pressure to the bulk system, or by growing it as a film. In this film form, KNO_3 has been proposed as a promising material for random-access memory devices.[1]

The unit cell of phase III KNO_3 is a five-atom rhombohedral cell with *R3m* symmetry as depicted in Fig. 1(a). This structure can be viewed as resulting from the stacking, along the rhombohedral axis, of planes consisting alternately of K atoms and NO_3 groups. However, it is found that a K plane is not equidistant from the NO_3 plane above it and the one below it. Instead, the system finds it favorable to adopt a polar structure in which the distance between a given K atom and its six O second-neighbors in the NO_3 plane below it is reduced at the expense of increasing the distance between this same K atom and its three O first-neighbors in the NO_3 plane above it [Fig. 1(d)]. Experimentally, the optimum stacking occurs when every K plane is roughly three times closer to the NO_3 plane below it than to the one above.[2] Of course, there must also exist a polarization-reversed structure having the same energy but with the K plane closer to the NO_3 plane above than to the one below. Moreover, the polarization reversal has to be accompanied by a NO_3 rotation of 60° in order to preserve the symmetry. The resulting structure is shown in Figs. 1(c) and (f). A paraelectric configuration that is intermediate between these two ferroelectric ones, having *R*32 symmetry, is shown in Fig. 1(b) and (e); in this case the K planes are equidistant from the NO_3 planes above and below, and each K atom has six equidistant O first neighbors. This structure is not found to be stable in nature, but corresponds to the saddle point on the energy surface connecting the degenerate minima. If we take the nitrate orientation in the case of Fig. 1(a) to correspond to an angle of $\theta = 0°$, then in the case of Fig. 1(b) we have $\theta = 30°$, and in the case of Fig. 1(c) we have $\theta = 60°$.

We presented preliminary results for ferroelectric KNO_3 as an illustrative example in a previous study in which we developed a formalism for carrying out first-principles calculations at constant polarization[3]. We obtained curves of energy E versus polarization P for polarizations parallel to the rhombohedral axis of KNO_3 using not only the full first-principles method, but also an earlier approximate approach introduced by Sai, Rabe, and Vanderbilt (SRV).[4] (The latter includes only the lattice-displacement responses to the electric field, while the method of Ref. 3 properly includes also the electronic contributions and is therefore exact.) We found that using the SRV method led to an $E(P)$ curve for KNO_3 that was smooth, with the orientation of the NO_3 group rotating continuously from $\theta = 0°$ to $\theta = 60°$. However, using the exact approach, we found a quite different $E(P)$ curve having a cusp at zero polarization, reflecting the presence of a discontinuity in $\theta(P)$ at $P = 0$. A brief discussion of this was given in Ref. 3, where these features were

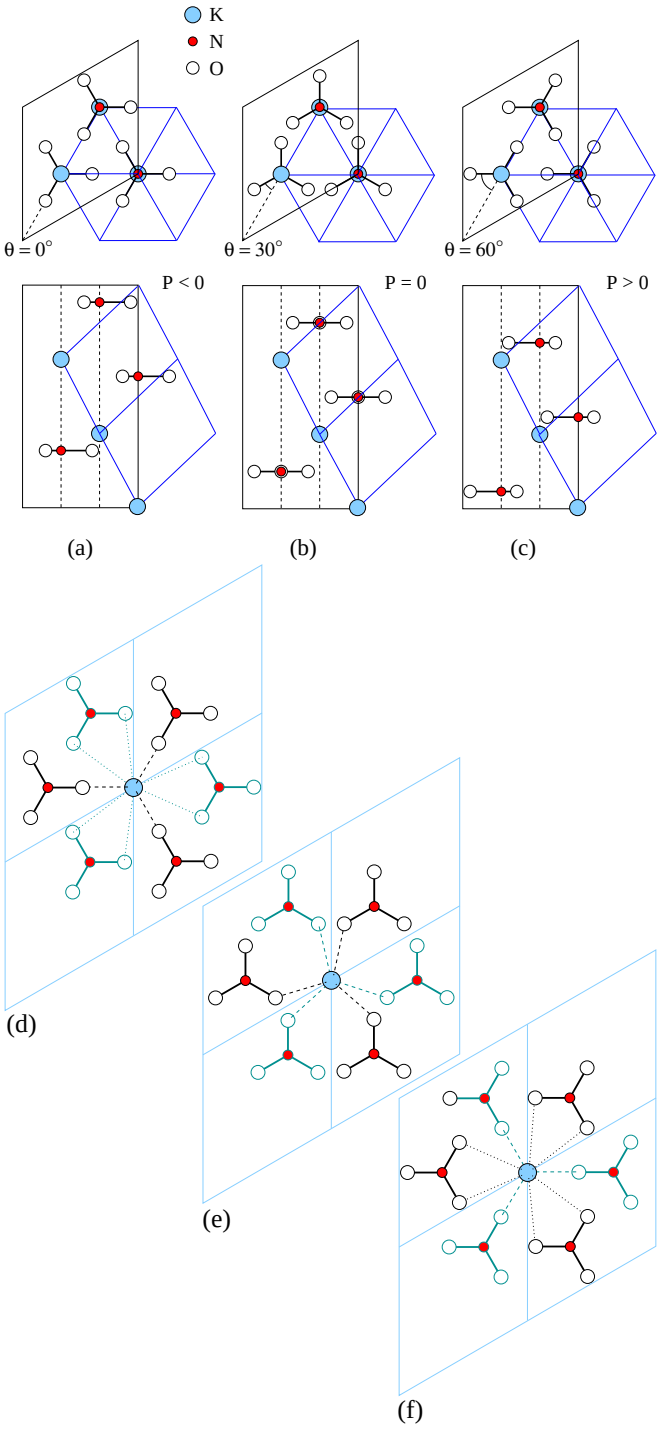

FIG. 1: (Color online) Top and side views of the fifteen-atom conventional hexagonal cell (outlined in black) for ferroelectric KNO_3 in (a) the ground state with negative polarization, (b) a metastable paraelectric state, and (c) the ground state with positive polarization. Blue lines indicate the equivalent five-atom rhombohedral cells. Panels (d)-(f) show top views of the same structures as in (a)-(c), clarifying the near-neighbor environment of a K atom. Neighbors in the plane above and below are indicated with black and blue lines respectively; first K-O neighbors are drawn as dashed lines, while second K-O neighbors are designated by dotted lines.

explained through the introduction of a simple model in which the energy of the system was expanded to low order in the relevant degrees of fredom (the polarization P and the nitrate group rotation angle θ).

The purpose of the present theoretical study is to investigate the structural and dielectric properties of phase III of KNO_3 in greater depth, and to provide a framework for understanding this and related systems. To do this, we combine extended first-principles calculations with a detailed analysis of the analytical model to be presented shortly. The picture that emerges is that of a system with a much richer variety of possible behaviors than can be found in conventional ferroelectrics. Some of these behaviors are realized for KNO_3 under external pressure, while others correspond to conditions that we have not reached in our first-principles calculations, but that could exist for related materials.

The rest of this article is organized as follows. In Sect. II we analyze the analytical model presented in Ref. 3. Section III contains first-principles results for the ferroelectric phase of KNO_3 under pressure. Finally, we summarize our results in Sect. IV.

II. ANALYTICAL MODEL

In the model introduced in Ref. 3, the energy may be written as

$$E(P,\theta) = E_0 + E^* \cos 6\theta + A\cos 12\theta + BP\cos 3\theta + CP^2 \quad (1)$$

where E^* serves as an energy scale for the definition of a dimensionless energy $\tilde{E} = (E - E_0)/E^*$. We also define a polarization scale $P^* = \sqrt{E^*/C}$ and a dimensionless polarization $\tilde{P} = P/P^*$, and rewrite Eq. (1) in rescaled form as

$$\tilde{E}(\tilde{P},\theta) = \cos 6\theta + \alpha\cos 12\theta + \beta\tilde{P}\cos 3\theta + \tilde{P}^2 \quad (2)$$

where

$$\alpha = \frac{A}{E^*} \quad (3)$$

and

$$\beta = \frac{B}{\sqrt{CE^*}} \quad (4)$$

are two dimensionless parameters determining the behavior of the model.

A. Phase diagram

We begin by analyzing in detail the possible behaviors that the model system of Eq. (2) can take as α and β are varied, thereby building up the phase diagram of Fig. 2.

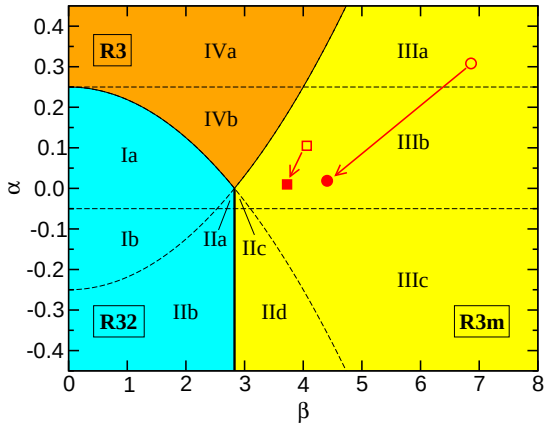

FIG. 2: (Color online) Phase diagram of the model given by Eq. (2) including a paraelectric phase ($R32$) and two ferroelectric phases ($R3m$ and $R3$). Each thick (thin) continuous line represents a first-order (second-order) phase transition. The broken lines enclose areas of the diagram mentioned in the text. The empty circle (square) corresponds to a fit of the exact (SRV) $E(P)$ fixed-cell first-principles calculations for KNO_3 to Eqs. (1-2); the filled symbols and the arrows indicate how the situation changes when stress in the cell is relaxed (zero pressure).

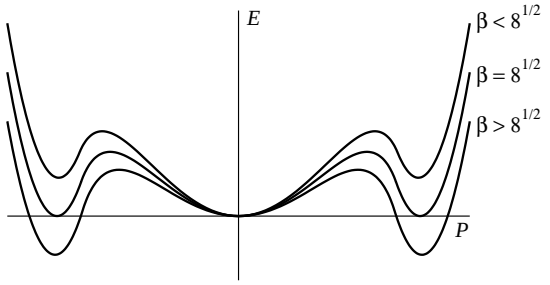

FIG. 3: Energy versus polarization curves in area IIa (top curve), area IIc (bottom curve), and on the boundary separating them (middle curve). The value of α is the same in all three cases; the system goes from paraelectric to ferroelectric with increasing β.

We will assume that $\beta > 0$, since the $\beta < 0$ case is equivalent to changing $\tilde{P}$ into $-\tilde{P}$. We identify the local minima of $E(\tilde{P}, \theta)$ on the basis of its first and second derivatives, arriving at the following classification. First, there is a minimum at ($\tilde{P} = 0$, $\theta = 30°$) iff $\alpha \leq (8 - \beta^2)/32$ (areas I and II in Fig. 2). Second, there are two equivalent minima at ($\tilde{P} = -\beta/2$, $\theta = 0°$) and ($\tilde{P} = +\beta/2$, $\theta = 60°$) iff $\alpha \geq (\beta^2 - 8)/32$ (areas II and III in Fig. 2). And third, there are two equivalent minima with rotation angles satisfying $\cos 6\theta = (\beta^2 - 8)/(32\alpha)$ and $\tilde{P} = -(\beta/2)\cos 3\theta$ iff $\alpha \geq (\beta^2 - 8)/32$ and $\alpha \geq (8 - \beta^2)/32$ (area IV in Fig. 2). Note that local minima of the first and second kind coexist in area II, and we subdivide this according to whether the the global minimum is of the first kind (for $\beta < 2\sqrt{2}$) or of the second kind (for $\beta > 2\sqrt{2}$). One is thus led to the phase diagram depicted in Fig. 2, showing three ground-state phases: a paraelectric $R32$ phase (area I and the left part of area II), a ferroelectric $R3$ phase (area IV), and a ferroelectric $R3m$ phase (the right part of area II and area III). The transition from phase $R32$ to $R3m$ is of first order, while the other transitions are of second order.

We establish a further subclassification of the areas in the diagram by considering whether or not the corresponding $\tilde{E}(\tilde{P})$ curves have continuous derivatives (or equivalently, whether or not $\theta(\tilde{P})$ remains continuous). It can be shown that this depends only on α. For $\alpha > 1/4$, there is a discontinuity in $\theta(\tilde{P})$ at $\tilde{P} = 0$, with the angle jumping from $30° - \theta_0$ to $30° + \theta_0$, where $0 < \theta_0 < 30°$. For $-1/20 < \alpha < 1/4$, $\theta(\tilde{P})$ is continuous and $\tilde{E}(\tilde{P})$ is smooth. Finally, for $\alpha < -1/20$ there is a discontinuity in $\theta(\tilde{P})$ at $\tilde{P} = -\tilde{P}'$ with θ jumping from 0 to θ', and another equivalent discontinuity at a positive $\tilde{P} = \tilde{P}'$ with θ jumping from 60° to $60° - \theta'$, where $\tilde{P}' > 0$ and a $0 < \theta' < 30°$. The areas that arise in this way have been labeled by appending a letter (a, b, c, or d) to the Roman numeral used in the main classification.

B. Triple-well potentials

A very interesting area of the phase diagram of Fig. 2 is area II, in which a minimum at ($\tilde{P} = 0$, $\theta = 30°$) coexists with the pair of equivalent minima at $\theta = 0°$ and $\theta = 60°$. It can be shown that if $\beta < 2\sqrt{2}$ then the paraelectric minima has the lowest energy, while if $\beta > 2\sqrt{2}$ the ferroelectric minima are energetically favoured. Curves of $\tilde{E}(\tilde{P})$ for both cases, as well as for the $\beta = 2\sqrt{2}$ case, are drawn in Fig. 3. They correspond to areas IIa and IIc, in which the derivative for each of them is continuous, and illustrate clearly the first-order character of the transition from the $R32$ phase to the $R3m$ phase. (Analogous curves can be found at areas IIb and IId, but in those cases there are two points at which the first-derivative of $\tilde{E}(\tilde{P})$ is not continuous.) These curves are similar to the ones that describe the free energy of a ferroelectric material at temperatures in the vicinity of a first-order paraelectric-ferroelectric transition (see, e.g., Ref. 6). However, we are not aware of any previous instance in which a first-principles mapping of energy versus polarization has revealed this kind of triple-well behavior at zero temperature.

C. Fitting previous first-principles results

The SRV results in Ref. 3 provide an example of a system showing a behavior that belongs in area IIIb, while the exact results case falls into area IIIa. Fitting the first-principles results to Eq. (1) and using the rescaling of Eq. (2), we find $\alpha = 0.105$ and $\beta = 4.06$ for the SRV case, while instead $\alpha = 0.308$ and $\beta = 6.86$ for the exact case. These points have been indicated in Fig. 2 with an empty

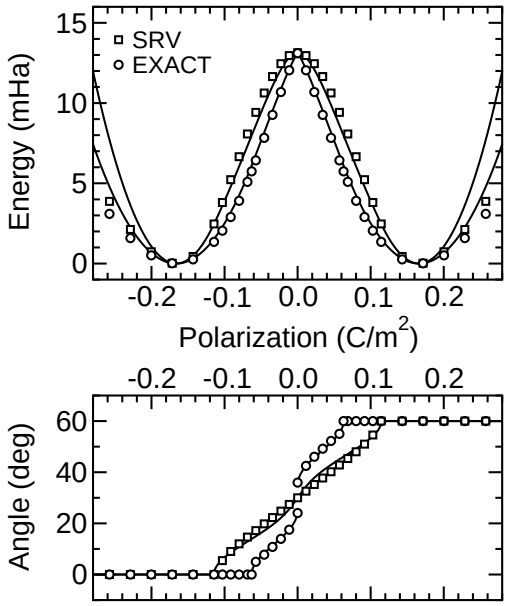

FIG. 4: Energy versus polarization, and NO_3 rotation angle versus polarization, for the ferroelectric phase of KNO_3 without strain relaxation. The squares and circles represent SRV and exact first-principles calculations respectively (from Ref. 3), while the curves have been fitted to these data using Eqs. (1-2) as described in the text.

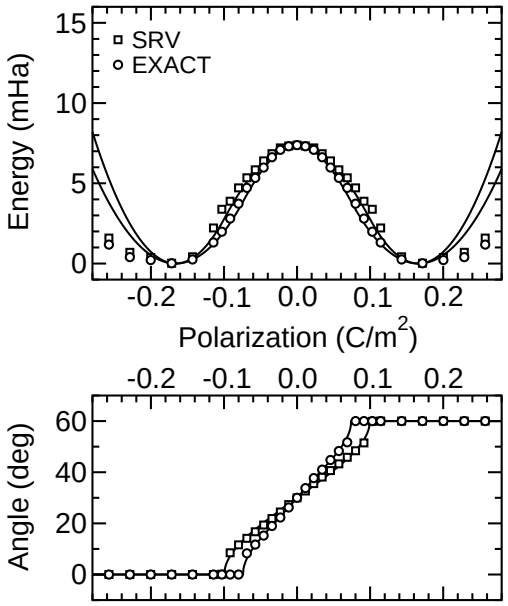

FIG. 5: Energy versus polarization, and NO_3 rotation angle versus polarization, for the ferroelectric phase of KNO_3 with strain relaxation. The squares and circles represent SRV and exact first-principles calculations respectively, while the curves have been fitted to these data using Eqs. (1-2) as described in the text.

square and circle, respectively. The model curves that result when these values are used, together with the points obtained from first-principles calculations, are plotted in Fig. 4. We can see that in the region between the two minima the fit is excellent, indicating that our relatively simple model captures the important $E(P)$ physics of the system. As the absolute magnitude of P grows too large, more powers of P are needed in the model to improve the fit. We have found that including terms up to fourth order works very well even for large values of P.

III. FIRST-PRINCIPLES RESULTS

A. Cell vectors relaxation

The calculations in Ref. 3 were carried out with the lattice vectors fixed to be those of the ground state, even when the polarization is varied away from its spontaneous value. It is also possible to relax the cell vectors;[11] we have now done that here, arriving at results valid for the more realistic situation of stress-free (i.e., zero-pressure) boundary conditions. As in our previous work,[3] we use density-functional theory[5] as implemented in the ABINIT code,[7] the local-density approximation (LDA),[8] a plane-wave cutoff of 30 Ha, a reciprocal space grid with 6 inequivalent points, and Troullier-Martins[9] pseudopotentials.[10]

The fitting parameters α and β resulting from these new calculations are shown in Fig. 2 as filled symbols, while the corresponding $E(P)$ and $\theta(P)$ curves are shown in Fig. 5. These values are compared with the ones for the non-relaxed case in Table I. The SRV results are similar to the ones in the non-relaxed case, apart from a reduction in the height of the double-well barrier that might have been expected in view of the additional degrees of freedom that are relaxed in the free-stress case. However, the exact results have changed qualitatively. The cusp at zero polarization and the corresponding discontinuity in the NO_3 rotation angle have now disappeared, and the exact curves are quite similar to the SRV ones. We have also found that as the polarization crosses through zero, the cell volume expands appreciably. Specifically, the rhombohedral lattice parameter goes from 7.62 a.u. in the ferroelectric ground state to 8.00 a.u. in the paralectric case (a 5% increase), with the rhombohedral angle going from 78.0° to 76.8°. This increase in lattice volume occurs so that the N-O bond length can keep similar values in the ferroelectric $R3m$ ground state (2.353 a.u.) and in

TABLE I: Values of the model parameters α and β depending on whether the cell vectors are relaxed or not, and whether we use the SRV method or the exact one.

	SRV		Exact	
	α	β	α	β
Fixed cell vectors	0.105	4.06	0.308	6.86
Relaxed cell vectors	0.010	3.72	0.019	4.41

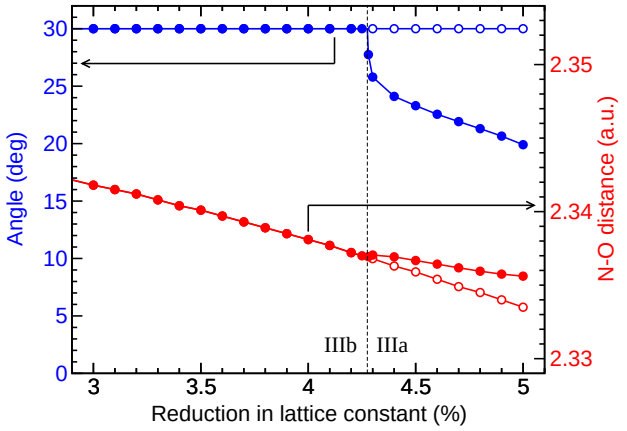

FIG. 6: (Color online) Zero-polarization first-principles calculations of the value of the NO_3 rotation angle and of the N-O distance in KNO_3 as functions of the reduction in the lattice parameter. The empty symbols correspond to calculations in which the $R32$ structure is imposed, while the the filled symbols correspond to calculations in which this restriction is removed. All calculations were done using the exact method of Ref. 3.

the less closely-packed paraelectric $R32$ state (2.351 a.u.). The reason for the appearance of the cusp at P=0 in the case of fixed lattice constants of 7.62 a.u. can be traced to the fact that the N-O bond distance becomes uncomfortably short at 2.337 a.u. if the $R32$ symmetry is enforced. Instead, the system prefers to lower its symmetry to $R3$ via a rotation of the nitrate groups (from $\theta = 30°$ to 36.1° or 23.9°, depending on whether $P \to 0^+$ or 0^-), with the N-O distance attaining a slightly larger length of 2.338 a.u.

B. Calculations under pressure

The description provided in the previous paragraph seems to indicate that if the ferroelectric phase of KNO_3 were compressed, we should expect to see the $E(P)$ cusp and $\theta(P)$ discontinuity at zero polarization reappearing at some value of applied pressure. To test this hypothesis, we have performed zero-polarization calculations for lattice parameters smaller than 8.00 a.u. while keeping the rhombohedral angle fixed at 76.8°. This is computationally simpler than doing calculations at constant pressure, and we have confirmed that the anisotropy in the stress tensor obtained in this way remains quite small (∼3 GPa at most), so that the rhombohedral angle would be expected to change very little if the rhombohedral angle were relaxed. The results, shown in Fig. 6, indicate that when the lattice parameter is reduced by around 4.3%, a cusp reappears in the $E(P)$ curve and the $R32$ structure becomes unstable to the $R3$ structure ($\theta \neq 30°$.) at $P = 0$. The figure also shows that the N-O bonds are not so tightly compressed as they would be at $\theta = 30°$. Therefore, we recover the IIIa and IIIb behaviors described in Ref. 3, but this time it is the pressure applied to the material that drives the transition between them.

IV. SUMMARY

To summarize, we report a theoretical study of the properties of ferroelectric phase III of KNO_3. We have carried out first-principles calculations that show that the polarization reversal mechanism in this material is accompanied by a rotation of 60° in the orientation of the nitrate groups. When the pressure exerted on the system is high enough, the corresponding double-well potential shows a distinctive cusp at zero polarization, and the mentioned rotation is discontinuous. These features are very well reproduced by a simple model in which the energy is expanded to low order in the polarization and the rotation angle of the nitrate groups. The phase diagram that arises from this model contains regions that can be realized by varying the pressure on ferroelectric KNO_3, as well as other regions that might turn out to be relevant for related materials in the future. One particularly interesting region of the phase diagram describes a system having a triple-well structure as a function of polarization, a feature not yet encountered in the context of first-principles studies of ferroelectric energy landscapes.

Acknowledgments

The authors thank J. Scott for suggesting the study of KNO_3. This work was supported by ONR Grant N0014-05-1-0054.

* Present address: *Massachusetts Institute of Technology, Department of Materials Science and Engineering, 77 Massachusetts Avenue, Cambridge MA 02139, USA.*

[1] J. F. Scott, M. S. Zhang, R. B. Godfrey, C. Araujo, and L. McMillan, Phys. Rev. B **35**, 4044 (1987).
[2] J. K. Nimmo and B. W. Lucas, Acta Cryst. B **32**, 1968 (1976).
[3] O. Diéguez and D. Vanderbilt, Phys. Rev. Lett. **96**, 056401 (2006).
[4] N. Sai, K. M. Rabe, and D. Vanderbilt, Phys. Rev. B **66**, 104108 (2002).
[5] P. Hohenberg and W. Kohn, Phys. Rev. **136**, B864 (1964).
[6] M. E. Lines and A. M. Glass, *Principles and Applications of Ferroelectrics and Related Materials* (Clarendon Press, Oxford, 1977).
[7] The ABINIT code is a common project of the Université Catholique de Louvain, Corning Incorporated, and other contributors (`www.abinit.org`). See: X. Gonze, J.-

M. Beuken, R. Caracas, F. Detraux, M. Fuchs, G.-M. Rignanese, L. Sindic, M. Verstraete, G. Zerah, F. Jollet, M. Torrent, A. Roy, M. Mikami, P. Ghosez, J.-Y. Raty, and D. C. Allan, Comp. Mat. Science **25**, 478 (2002).

[8] D. M. Ceperley and B. J. Alder, Phys. Rev. Lett. **45**, 566 (1980).

[9] N. Troullier and J. L. Martins, Phys. Rev. B **43**, 1993 (1991).

[10] The pseudopotentials files used are available at: `www.abinit.org/Psps/?text=../Psps/LDA_FHI/fhi`.

[11] X. Wu, M. Stengel, K. M. Rabe, and D. Vanderbilt, in preparation.